

CHAPTER 3

Factors that drive the geographical variability of the haploid:diploid ratio of biphasic life cycles

Published in Journal of Phycology (Vieira and Santos 2012).

ABSTRACT

The relative abundance of haploid and diploid individuals (H:D) of isomorphic biphasic life species varies spatially. This is only possible if the vital rates of isomorphic haploids and diploids vary differently with environmental conditions, i.e. if there is conditional differentiation between phases. The performance of the vital rates of isomorphic phases at a particular environment may be determined by subtle morphological or by physiological differences as described for marine algae.

Here we test numerically how the conditional differentiation of phases of isomorphic life cycles, i.e. vital rate dissimilarities between phases, and the type of life strategy of populations, i.e. life-cycles dominated by reproduction, survival or growth, determine the variability of H:D, i.e. the observed spatial variability. Simulation conditions were selected using the available data on the H:D spatial variability of seaweed species.

For species that evolved a life strategy of investment either in fertility or in growth a conditional differentiation between ploidy phases affecting whatever vital rates and paths had a small effect in the H:D variability. As opposed to both fertility and growth dominated life cycles, in species that evolved a life strategy of investment mainly in survival, an outstanding variability of the H:D was obtained with a conditional differentiation in stasis (the probability of staying in the same size class), breakage (the probability of changing to a smaller size class) or growth (the probability of changing to a bigger size class). The simulations of conditional differentiation developed in this work obtained values of H:D variability highly consistent with the observed spatial variability of the H:D of natural populations of marine algae.

Keywords: Biphasic life cycle; demography; geographical variability; H:D; haploid-diploid; ploidy ratio; population dynamics; spatial variability.

INTRODUCTION

Isomorphic biphasic life cycles are characterized by having two independent ploidy phases, which are morphologically identical and tend to overlap their niches. Hughes and Otto (1999) suggested that these phases should adapt differently to the environment in order for the biphasic life cycle to prevail. This is known as “conditional differentiation”. Haploids will tend to perform better at a specific vital rate whereas diploids will tend to perform better at another. Hughes and Otto (1999) demonstrated that minor differences in survival rates are sufficient for the biphasic life cycle to prevail, whereas in the first chapter it was demonstrated that these minor differences are enough to drive haploid to diploid ratios of abundances (H:D) highly deviated from 1.

The performance of the vital rates of isomorphic life cycle phases at a particular environment depends on subtle morphological or on physiological adaptations of the ploidy phases. For example, Santos and Duarte (1996) found tetrasporophytic fronds of the isomorphic rhodophyte species *Gelidium sesquipedale* to be longer and less branched than the isomorphic gametophytic fronds, while Lewis and Lanker (2004) found differences in branch angle and a tendency for dichotomy vs proliferative primary branches in *Ceramium codicola*. Carrington et al (2001) found that the kappa-type carrageenans of the gametophytes' distal tissue of *Chondrus crispus* make them stronger, more extensible and stiffer than the tetrasporophytes' distal tissue composed of weaker nongelling lambda-type carrageenans. They further argue that the kappa-type carrageenans may also render gametophytes more resistant to desiccation and herbivory. Thornber et al (2006) tested for herbivore selectivity among tissue types of the isomorphic red alga *Mazzaella flaccida* and found important differential grazing by snails for gametophyte reproductive tissue over other tissue types. The above features may result in differential survival rates between phases thus affecting the relative abundance of ploidy phases, i.e. the haploids to diploids ratio (H:D). The second chapter revealed that the H:D of biphasic life cycles is particularly responsive to ploidy phase dissimilarities, in particular to looping transitions (survival, breakage and clonal growth), when the life strategy is characterized by low fertility. Otherwise, dissimilarities between ploidy phases must be high to deviate H:D from 1.

Spatially separated populations of a species are subjected to different environmental conditions, which originate site specific patterns of vital rate dissimilarities between phases determined by conditional differentiation of phases. Consequently, the relative abundance of phases may vary spatially. Evidence for the spatial variability of the H:D was given by Engel et al (2001), Mudge and Scrosati (2003), Thornber and Gaines (2003) and Scrosati and Mudge (2004). The objective of this work is to evaluate how the conditional differentiation of phases of biphasic life cycles, i.e. vital rate dissimilarities between phases, and the type of life strategy, i.e. life cycles dominated by reproduction, survival or growth, determine the variability of H:D, i.e. the observed spatial variability. Numerical simulations were done to test the effects of dissimilarities of fecundity, growth and survival rates on H:D variability. Simulation conditions were selected using the H:D spatial variability data obtained by Engel et al.(2001) and Thornber and Gaines (2003)

METHODS

One set of one thousand theoretical populations was used in simulations to test the effects of life cycle phase dissimilarities of fecundity, growth and survival rates on H:D variability. In accordance with the second chapter, the H:Ds were calculated based on the phase ratios of three co-occurring pathways of frond fate, the fertility (F), the Growth (G) and the Looping (L) paths. The variability of the H:D (the dependent variable) and how much of that variability is explained by the variability of each path ratio (error propagation of the independent variables), was estimated through a Taylor transformation (Taylor 1955) of the analytical solution of the H:D using the stage/size structured model previously developed in the second chapter. All model implementation and analysis was done by software developed by the authors in Matlab environment.

The demographic model

The demographic matrices of populations are based on a stage/size structured model (matrix 1) where tetraspores (tet) develop into gametophytes and carpospores (carp) develop into tetrasporophytes. Gametophytes and tetrasporophytes were divided into three size classes (1, 2 and 3 and 4, 5 and 6, respectively). In each phase, individuals

flow among size classes through growth (g) or looping (l) transitions, which include stasis (staying in the same class) and breakage. When a value for Looping was attributed, it had to be determined how that value would be distributed among the vital rates stasis and breakage. The coefficient ‘a’ sets the fraction of Looping determined by breakage and 1-a that determined by stasis. The upper left and the lower right submatrices describe the within phase dynamics (gametophyte and tetrasporophyte phases, respectively) whereas the lower left and upper right matrices describe the fecundity dynamics of the gametophyte and tetrasporophyte phases, respectively. Fecundity transitions are those from size classes 1-3 to carpospores (carp) and from 4-6 to tetraspores (tet).

In the second chapter it was demonstrated that the elasticities of H:D to the vital rates are highly dependent on fertility. Therefore, the current analysis was performed for a wide range of fertilities. A spore survival (sp) ranging from 10^{-1} to 10^{-8} , but equal between phases, was randomly assigned to each of one thousand population matrices. The values of vital rates of the one thousand numerical simulations were developed to adjust the observations of Thornber and Gaines (2003) of a set of 6 geographically separated populations of *Mazzaella laminarioides*. The average H:D observed in these populations was 4. Because the H:D is given by the square root of the fertility ratio when all the other transitions are equal between phases (Scrosati and DeWreede 1999, Thornber and Gaines 2003 and second chapter), the fecundities of tetrasporophytes were considered 16 times higher than those of gametophytes. The growth (g) and looping (l) rates of size classes were randomly selected between 0 and 1 and the coefficient ‘a’ between 0 and 0.5. Dissimilarities between phases were then imposed on these vital rates.

The matrix M1 (equation 1) sets the vital rates under the assumption of ecological similarity. It implies that the fate of ramets (survival, growth, stasis and breakage) is equal between phases). The matrix M2 (equation 2) simulates the environmentally dependent dissimilarities between phases attributable to conditional differentiation. The final demographic matrix (A) was the Hadamard product of matrices M1 and M2 ($A = M1 \otimes M2$). This product is the element-wise product where element $M1_{i,j}$ only multiplies by element $M2_{i,j}$. The demographic model assumptions were that the estimated population growth rate (λ) was neither lower than 1 nor greater than 1.1, whereas survival in each size class was not greater than 1. Thus, any simulation where matrix A felled outside this range was rejected. These

assumptions were made to restrict the large range of possible mathematical outcomes to those that are more probable to occur in natural populations.

In order to create matrix M2 the dissimilarities between the vital rates of both phases (dx) were randomly selected from 0 to a maximum (dx_{max}) of 5% (that is from 0 to 0.05). These are only subtle dissimilarities, but they may have significant effects on H:D (second chapter). Three dissimilarity vectors were created, df for fertility, dg for growth and dl for looping transitions, with the form of $[1-dx/2 \ 1+dx/2]$. For each vital rate in each demographic matrix it was randomly chosen whether the dissimilarity would benefit the gametophytes or tetrasporophytes. To do so, the three dissimilarity vectors were independently randomly permuted before being introduced into the dissimilarity matrix M2.

$$M1 = \begin{bmatrix} & \begin{array}{c} tet \\ 1 \\ 2 \\ 3 \\ carp \\ 4 \\ 5 \\ 6 \end{array} & \begin{array}{c} tet \\ sp \\ g \\ 0 \\ fec_1 \\ 0 \\ 0 \\ 0 \end{array} & \begin{array}{c} 1 \\ l \\ g \\ 0 \\ fec_2 \\ 0 \\ 0 \\ 0 \end{array} & \begin{array}{c} 2 \\ l \times a \\ l \times (1-a) \\ g \\ fec_3 \\ 0 \\ l \times (1-a) \\ 0 \end{array} & \begin{array}{c} 3 \\ \frac{l \times a}{2} \\ \frac{l \times a}{2} \\ l \times (1-a) \\ fec_4 \\ 0 \\ 0 \\ 0 \end{array} & \begin{array}{c} carp \\ 0 \\ 0 \\ 0 \\ 0 \\ sp \\ 0 \\ 0 \end{array} & \begin{array}{c} 4 \\ fec_4 \\ 0 \\ 0 \\ 0 \\ l \\ g \\ 0 \end{array} & \begin{array}{c} 5 \\ fec_5 \\ 0 \\ 0 \\ 0 \\ l \times a \\ l \times (1-a) \\ g \end{array} & \begin{array}{c} 6 \\ fec_6 \\ 0 \\ 0 \\ 0 \\ \frac{l \times a}{2} \\ \frac{l \times a}{2} \\ l \times (1-a) \end{array} \end{bmatrix} \quad (eqn.1)$$

$$M2 = \begin{bmatrix} & \begin{array}{c} tet \\ 1 \\ 2 \\ 3 \\ carp \\ 4 \\ 5 \\ 6 \end{array} & \begin{array}{c} tet \\ 1 \\ 0 \\ 0 \\ 0 \\ 0 \\ 0 \\ 0 \end{array} & \begin{array}{c} 1 \\ dl_1 \\ dg_1 \\ 0 \\ df_1 \\ 0 \\ 0 \\ 0 \end{array} & \begin{array}{c} 2 \\ dl_1 \\ dl_1 \\ dg_1 \\ df_1 \\ 0 \\ 0 \\ 0 \end{array} & \begin{array}{c} 3 \\ dl_1 \\ dl_1 \\ dl_1 \\ df_1 \\ 0 \\ 0 \\ 0 \end{array} & \begin{array}{c} carp \\ 0 \\ 0 \\ 0 \\ 0 \\ 1 \\ 0 \\ 0 \end{array} & \begin{array}{c} 4 \\ df_2 \\ 0 \\ 0 \\ 0 \\ dl_2 \\ dg_2 \\ 0 \end{array} & \begin{array}{c} 5 \\ df_2 \\ 0 \\ 0 \\ 0 \\ dl_2 \\ dl_2 \\ dl_2 \end{array} & \begin{array}{c} 6 \\ df_2 \\ 0 \\ 0 \\ 0 \\ dl_2 \\ dl_2 \\ dl_2 \end{array} \end{bmatrix} \quad (eqn.2)$$

The demographic metrics estimated for each population were:

- the population growth rate (λ)
- the analytical solution to the H:D and its three components Q_G , Q_F and Q_L (from the second chapter).
- the investment in fertility (f) given by $sp \cdot \sum(fec_i \cdot n_i) / \sum n_i$, where n_i is the estimated abundance of size class i with the population in its stable structure. This is the average number of recruits at time t+1 produce by each individual at time t.

- the investment in growth (g). This is the average number of individuals that grew from time t to time t+1.
- the investment in looping (l). This is the average number of individuals that suffered a looping transition from time t to time t+1.
- the elasticities of the H:D to fertility (F), growth (G) and looping (L), given respectively by the sum of the absolute values of the elasticities of the H:D to the demographic matrix entries related to F, G and L. These elasticities were estimated by their analytical solutions derived as in the second chapter.

Analytical solution to the H:D

The demographic matrix A is primitive and irreducible and thus tends asymptotically to an ergodic population structure (Caswell 2001, Otto and Day 2007). Likewise, the H:D has the same behaviour, as shown in the second chapter. The analytical solution of the H:D adapted from the second chapter to the present is $H:D=Q_F*Q_G*Q_L$, where Q_F is the fertility path ratio given by equation 3, Q_G is the growth path ratio given by equation 4, Q_L is the looping path ratio given by equation 5 and where λ is the asymptotic population growth rate. The vital rates in these equations come from the demographic matrix A, which is the Hadamard product of M1 and M2, where: $g_G=g*dg_1$, $g_T=g*dg_2$, $l_G=l*dl_1$, $l_T=l*dl_2$, $f_1=fec_1*df_1$, $f_2=fec_2*df_1$, $f_3=fec_3*df_1$, $f_4=fec_4*df_2$, $f_5=fec_5*df_2$ and $f_6=fec_6*df_2$.

$$Q_G = \frac{(\lambda - l_G(1-a))^2 - g_G \left(\lambda + l_G \cdot \frac{a-2}{2} + g_G \right)}{(\lambda - l_T(1-a))^2 - g_T \left(\lambda + l_T \cdot \frac{a-2}{2} + g_T \right)} \quad (\text{eqn.3})$$

$$Q_F = \sqrt{\frac{fec_4 \left[(\lambda - l_T(1-a))^2 - g_T \cdot b_T \cdot \frac{a}{2} \right] + g_T \cdot [fec_5 \cdot (\lambda - l_T(1-a)) + fec_6 \cdot g_T]}{fec_1 \left[(\lambda - l_G(1-a))^2 - g_G \cdot b_G \cdot \frac{a}{2} \right] + g_G \cdot [fec_2 \cdot (\lambda - l_G(1-a)) + fec_3 \cdot g_G]}} \quad (\text{eqn.4})$$

$$Q_L = \sqrt{\frac{\left[(\lambda - l_T(1-a))^2 - g_T \cdot l_T \cdot \frac{a}{2} \right] \cdot (\lambda - l_T) - g_T \cdot l_T \cdot a \cdot \left(\lambda - l_T(1-a) + \frac{g_T \cdot l_T}{2} \right)}{\left[(\lambda - l_G(1-a))^2 - g_G \cdot l_G \cdot \frac{a}{2} \right] \cdot (\lambda - l_G) - g_G \cdot l_G \cdot a \cdot \left(\lambda - l_G(1-a) + \frac{g_G \cdot l_G}{2} \right)}} \quad (\text{eqn.5})$$

Error propagation

One thousand different populations were simulated. These were split into nine subsets, each representing a different level in the gradient from fertility to survival dominated demographics. Within each subset both the average H:D and the error around it were estimated. Since the H:D is a function of the vital rates, the error around the average H:D is also a function of the error around the average vital rates. This function was derived with using a Taylor expansion of the analytical solution to the H:D. Within each subset, it was thus possible to determine exactly how much error was associated to each vital rate and how it flew through the demographic model to generate a precise amount of variation around the H:D. However, estimating each error flow for all the vital rates would be too extensive. A simpler alternative was estimating the amount of error in each path ratio (Q_F , Q_G and Q_L) and how these propagated to yield the H:D final error. Equation 6 was obtained applying the same methodology, where the first three terms described the propagation of the total error in each path ratio. These were named “err Q_G ”, “err Q_F ” and “err Q_L ”. The last three terms, “err Q_GQ_F ”, “err Q_GQ_L ” and “err Q_FQ_L ”, described the propagation of the error shared within each pair of path ratios. In order not to be accounted twice these needed to be subtracted and thus always had negative values. Appendix III shows the detailed deduction of the analytical solution to the propagation of the error in Q_G , Q_F and Q_L to the error in H:D.

$$\begin{aligned} \text{var}(H : D) = & \text{var}(Q_G)(Q_F \cdot Q_L)^2 + \text{var}(Q_F)(Q_G \cdot Q_L)^2 + \text{var}(Q_L)(Q_G \cdot Q_F)^2 + \\ & + 2 \cdot \text{cov}(Q_G, Q_F)Q_G \cdot Q_F \cdot Q_L^2 + 2 \cdot \text{cov}(Q_G, Q_L)Q_G \cdot Q_F^2 \cdot Q_L + 2 \cdot \text{cov}(Q_F, Q_L)Q_G^2 \cdot Q_F \cdot Q_L \end{aligned} \quad (\text{eqn.6})$$

Application to case studies

New simulations were done changing the maximum dissimilarity coefficients between phases (dx_{\max} of df , dg and dl) separately and in an amount that would give the best fit between the simulated and the observed H:Ds for a subset of 30 populations. The mean and variances of the H:Ds of each subset were compared to those of the natural populations of algae observed by Engel *et al* (2001) and Thornber and Gaines (2003). The geometric mean and variance were used to compare observed and simulated H:Ds instead of the arithmetic mean and variance because the H:D is a ratio. To illustrate

why, assume a population with even abundances of 3:3 where the overall H:D is 1. If the population is divided into two subpopulations with uneven abundances of 2:1 and 1:2, the arithmetic mean yields $\mu=1.25$, whereas the geometric mean yields $\mu=1$. The geometric variance (equations 8a) was estimated using the geometric mean (equation 7a) and geometric bias (equation 7b). The same principle of geometric mean and bias could not be used in the previous analysis about the error propagation because the algebraic scheme of the Taylor expansion relies on the arithmetic differential (differential is a bias).

$$\mu = \sqrt[n]{\prod_i x_i} \quad (\text{eqn.7a}) \quad \text{bias}_i = \ln\left(\frac{x_i}{\mu}\right) \quad (\text{eqn.7b})$$

$$\text{var}_x = \frac{1}{n-1} \sum_i \text{bias}_{x,i}^2 \quad (\text{eqn.8a}) \quad \text{cov}_{x,y} = \frac{1}{n-1} \sum_i (\text{bias}_{x,i} \cdot \text{bias}_{y,i}) \quad (\text{eqn.8b})$$

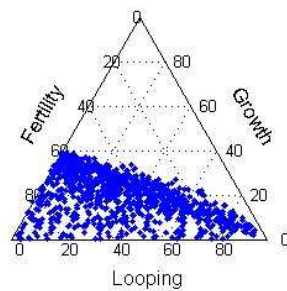
RESULTS

The elasticity of a demographic trait (such as λ or the H:D) to a vital rate (or to a group or type of vital rates) is a measure of the effect of that vital rate on that demographic trait. To visualize the relative importance of the groups of vital rates, F; G and L in determining the population growth rate, λ , and the H:D, one thousand simulated populations were mapped in a triplot according to the λ elasticities to F, G and L (Fig.1 top) and the H:D elasticities to F, G and L (Fig.1 bottom). An evident gradient from dominance of the elasticity to F to the dominance of the elasticity to L is revealed, and also that populations are never very elastic to G, particularly when the elasticity of λ to L increases and that to F decreases.

The same plotting was done imposing a gray scale for the populations' investments in Fertility (F), Growth (G) and Looping (L) (Fig.2). It became evident that as populations' strategies shift from investment in fertility (Fig.2, darker F gray scale) to investment in growth (Fig.2, darker G gray scale) to investment in looping (Fig.2, darker L gray scale), their demographic traits (λ and H:D) shift from being determined by fertility (Fig.2, darker F gray scale close to the corner with 100%

elasticity to F) to being determined by looping (Fig.2, darker L gray scale close to the corner with 100% elasticity to L) and that they never become much determined by growth, even in the populations where growth rates are highly dominant over fertility and looping rates (Fig.2, darker G gray scale far from the corner with 100% elasticity to G). In these populations, their demography, particularly the H:D, is always also very influenced by either F or L.

% of the elasticities of lambda to F, G and L



% of the elasticities of the H:D to F, G and L

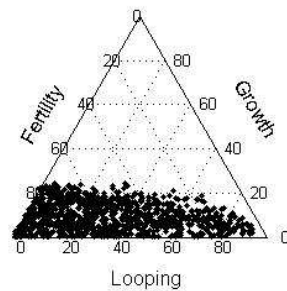


Figure 1. - Relative importance (% elasticities) of the vital rate categories, fertility (F), growth (G) or looping (L) of one thousand simulated populations, in determining the population growth rate, λ , (top) and the H:D (bottom). Axis coordinates: sum of the absolute values of the elasticities to all the vital rates belonging to a category divided by the sum of the absolute values of all the elasticities.

Another major difference between the life strategies dominated by fertility and those dominated by looping was found. In populations where the H:D is dominated by fertility, all elasticities are low and thus also is their total sum (left corner of Fig.3). In this case, none of the vital rates has a great effect on the H:D. On the other hand, in populations where the H:D is determined by looping (those of the right corner of Fig.3) all elasticities are moderate to high and thus their sum is very high. In this case, small variations in the vital rates have drastic impacts on the H:D.

Elasticities of Lambda to F, G, and L

Elasticities of H:D to F, G and L

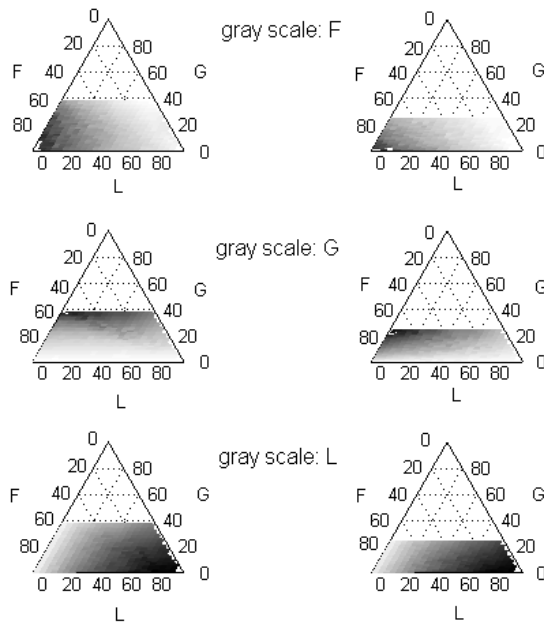


Figure 2- Same plotting of Figure 1, but the investment of the simulated populations in a vital rate category fertility (F), growth (G) or looping (L) (sum of the parameter values of that category) is given by the gray scale: maximum in darker and minimum in lighter.

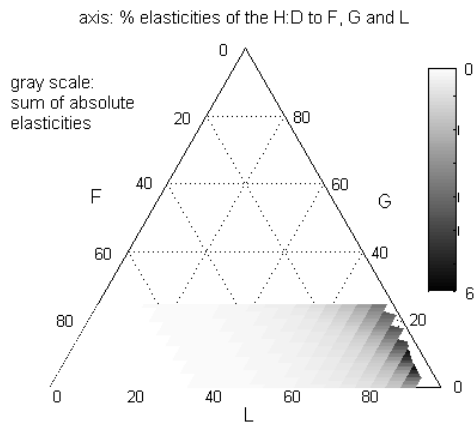


Figure 3. Relation between life strategy and the H:D overall susceptibility to change. Same plotting of Figure 2, but the colour scale represents the sum of the absolute values of the elasticities to all the vital rates, ith maximum in darker and minimum in lighter.

As previously mentioned in Methods, nine subsets of populations were created to analyse the error propagation (Fig 4). These only include the gradient from populations with fertility dominated life-strategies to populations with survival (looping) dominated life-strategies. Populations with growth dominated life-strategies were also analyzed but they were not reported for simplicity as they showed identical behaviour and no further relevant information was added. Each of the nine subsets analysed include all the populations inside each of the dotted triangles along the bottom axis (L axis) of Figure 1- bottom, with subset '1' being in the left corner (populations where H:D is mainly determined by fertility) and stepping forward to

subset '9' in the right corner (populations where H:D is mainly determined by looping). From subset 1 to subset 9, the error around the H:D increased greatly (Fig.4). This increase is mostly due to the increasing propagation of the error through the looping path (Q_L). The increase of the propagation of the error through the growth path (Q_G) was far less and the propagation of the error through the fertility path (Q_F) was irrelevant. This error was obtained with a maximum 5% dissimilarity imposed to any type of vital rates and randomly choosing (independently among types of vital rates) whether it was the gametophyte or tetrasporophyte rates to benefit from the dissimilarity. In order to have a clearer notion of what this error meant in terms of H:D variability a boxplot was made with the quartiles of the H:D distribution for each subset of populations (Fig.5). The subset most dominated by looping presented H:Ds ranging from 1.73 to 6.71 ($n = 43$ populations), whereas the subset most dominated by fertility presented H:Ds ranging from 3.87 to 4.14 ($n = 178$ populations).

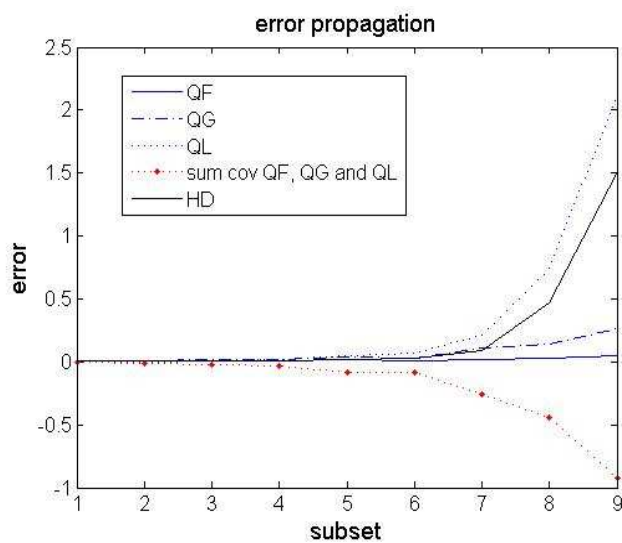


Figure 4 - Error propagation of the nine subsets of simulated population from fertility dominated (subset 1) to looping dominated life cycles (subset 9). The variance of H:D is disaggregated into the variances of its components, quotients Q_F , Q_G and Q_L , and into the covariances between quotients.

Application to case studies

Thornber and Gaines (2003) studied the temporal and spatial variability of the H:Ds of *Mazzaella splendens* and *Mazzaella flacida*, in the west coast of USA, *Mazzaella laminarioides*, in Chile and *Mazzaella capensis*, in South Africa. The H:D of the six *M. laminarioides* populations showed marginally significant variation between years and a significant spatial variation. These values are similar to those obtained for populations of subset 9 (Fig.5), in which the H:D is mostly determined by

dissimilarities in survival rates (both looping and growth rates) (Fig.4). The geometric mean of the H:Ds of *M. laminarioides* populations was 4.05 and the geometric variance was 0.227, quite similar values to the geometric mean and variance (3.99 and 0.214, respectively) of 30 theoretical populations included in subset 9 with 5.5% of dissimilarities imposed ($dx_{\max}=0.055$). In order to obtain similar results due to dissimilarities in fertility a dissimilarity of 300% ($dx_{\max}=3$) had to be imposed to 30 populations belonging to subset 1, in which the H:D is mostly determined by fertility. Then, an H:D geometric mean of 4.32, with a geometric variance of 2.18, were obtained.

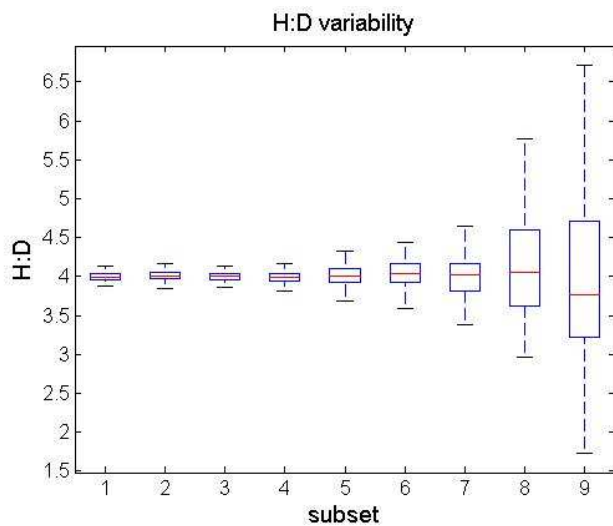


Figure 5 - Box plots of H:D distribution (quartiles) of the nine subsets of simulated populations, from fertility dominated life cycles (subset 1) to looping dominated life cycles (subset 9).

The H:D values of the seven *Mazzaella flaccida* populations studied by Thornber and Gaines (2003) showed a significant spatial variation. However, they did not show a significant variation among the four years of the study, suggesting this space variation to be stable in time. The site specific geometric mean was 3.01 and the geometric variance was 0.303. To attain similar simulated values of H:D, a 7.3% dissimilarity ($dx_{\max}=0.073$) and a tetrasporophyte fecundity 9 times higher than gametophyte fecundity had to be imposed to 30 simulated populations belonging to subset 9. Then, a geometric mean of 2.95 and a geometric variance of 0.314 were obtained. In order to obtain similar results due to dissimilarities in fertility it had to be simulated 30 populations belonging to subset 1. Then, a dissimilarity of 485% ($dx_{\max}=4.85$) yielded a geometric mean of 3.16 and a geometric variance of 2.97.

Also the *Mazzaella Splendens* populations studied by Thornber and Gaines (2003) showed no significant variation among years but did show a significant spatial variation. The geometric mean was 1.67 and the geometric variance was 0.464. It is more variable than the results from 30 populations simulated as belonging to subset 9, with 10% dissimilarities imposed ($dx_{\max}=0.1$) and with tetrasporophyte fecundity manipulated to 2.79 times higher than gametophyte fecundity. In this simulation the geometric mean was 1.49 and the geometric variance was 0.15. Higher dissimilarities were not imposed in this case because it was very hard to generate demographic matrices acceptable over all predefined criteria. In order to obtain results similar to the observations due to dissimilarities in fertility it had to be simulated 30 populations belonging to subset 1. Then, a dissimilarity of 550% ($dx_{\max}=5.5$) yielded a geometric mean of 1.34 and geometric variance 0.48.

The *Mazzaella capensis* studied by Thornber and Gaines (2003) was the only species that did not showed significant variation among sites with the H:D ranging from 1.48 at Elands Bay to 1.97 at Kommetjie. Unfortunately the authors did not publish any further information about the H:D at the other three sampled sites.

Engel *et al.* (2001), found four populations of *Gracilaria gracilis* from northern France to have survival dominated life strategies with average stage survival rates between 95% and 98%, low recruitment rates with average $5.29 \text{ recruits} \cdot \text{stage}^{-1} \cdot \text{year}^{-1}$, generation times between 12 and 42 years and the populations' dynamics to be much more elastic to survival rates than to other types of rate. The reasonable temporal constancy of the four populations suggests they could be close to steady-state and hence fall into the premises of the present work. Both Audresselles low inter-tidal (AuL) and high inter-tidal (AuH) populations had balanced phases abundances (between 49% and 53% tetrasporophytes corresponding to H:D from 1.04 to 0.89). On the contrary, the Cape Gris-Nez high inter-tidal (GNH) population exhibited a gametophyte dominance (between 44% and 46% tetrasporophytes corresponding to H:D from 1.27 to 1.17) while the Cape Gris-Nez low intertidal (GNL) population exhibited a tetrasporophyte dominance (between 59% and 63% tetrasporophytes corresponding to H:D from 0.69 to 0.59). The geometric mean H:D for each of the populations was respectively AuH= 0.92, AuL=0.94, GNH=1.21 and GNL=0.64. The overall geometric mean of the H:D was 0.90 and the geometric variance was 0.069. A similar H:D geometric mean and variance was obtained in 30 simulated populations belonging to subset 8, imposing a

16% maximum dissimilarities ($dx_{\max}=0.16$) between survival related rates (growth and looping) and with tetrasporophyte fecundity manipulated to 0.81 times the gametophyte fecundity. Subset 8 was looping dominated where the looping path was responsible for the bulk of the error propagation (Fig.4). For this simulation the geometric mean was 0.88 and the geometric variance was 0.066. A similar H:D variance was obtained also for 30 simulated populations belonging to subset 9, imposing a 5% maximum dissimilarities ($dx_{\max}=0.05$) between survival related rates. Then, the geometric mean was 0.91 and the geometric variance was 0.07. Finally, a similar H:D variance was obtained for 30 simulated populations belonging to subset 1, imposing a 83% maximum dissimilarities ($dx_{\max}=0.83$) between fertility rates. Then, the geometric mean was 0.91 and the geometric variance was 0.065.

DISCUSSION

This work successfully simulated a conditional differentiation (*sensu* Hughes and Otto 1999) among the different types of vital rates, which is likely to be driven by different environmental factors or combinations of factors. Even small scale differences in the spatial distribution of algae may determine highly different exposures to factors such as light, hydrodynamics and grazing, which may strongly affect their vital rates. In the specific case of algae with biphasic life-cycles, even in the case of isomorphic ones, specific phase responses to environmental factors have been widely reported (Carmona and Santos 2006, Destombe et al 1989, Engel et al 2001, Gonzalez and Meneses 1996, Thornber and Gaines 2004, Thornber 2006). The simulations of conditional differentiation developed in this work obtained values of H:D variability highly consistent with the observed spatial variability of the H:D reported for *Gracilaria gracilis* (Engel et al 2001), *Mazzaella flaccida*, *Mazzaella laminarioides* and *Mazzaella splendens* (Thornber and Gaines 2003).

The expected amount of H:D variability of a species depends on the type of life strategy, i.e. on the relative importance of the three different types of vital rates and their paths of fertility, growth and looping, where growth and looping add up to survival. For species that evolved a life strategy of investment mainly in fertility, with low survival rates, low generation times and high turnover rates, a conditional differentiation between ploidy phases affecting whatever vital rates and paths had a

small effect in the H:D variability. This extends the knowledge of the H:D dynamics obtained in the previous chapter, who showed that the H:D of species dominated by fertility are little elastic to changes in any vital rate or path. Also for the species which demography is dominated by growth, a conditional differentiation over any type of vital rate or path will have little effect on the H:D and thus on its spatial variability. As opposed to both fertility and growth dominated life cycles, in species that evolved a life strategy of investment mainly in survival, with high survival rates, high generation times and low turnover rates, an outstanding variability of the H:D was obtained with a conditional differentiation of the looping path between ploidy phases. Even low dissimilarities in survival between the life cycle phases surge throughout the life-cycle generating highly deviated H:Ds. These highly deviated H:Ds could only be obtained when imposing dissimilarities between ploidy phase in stasis (the probability of staying in the same size class), breakage (the probability of changing to a smaller size class) and growth (the probability of changing to a bigger size class). The previous chapter showed that, in species dominated by survival, the H:D is highly elastic to changes in looping rates (stasis, breakage and clonal growth).

In Fierst et al (2005) and in the second chapter it was already determined the strong dependency of the H:D dynamics from the type of life strategy by imposing widely different fertilization rates. But while Fierst et al (2005) did not explicitly assumed it as simulating different life strategies, the second chapter did so. The present work further reveals the importance of the type of life strategy in setting an H:D spatial variability in any given biphasic life-cycle algal species

The simulated H:D variability patterns fitted very well the observed patterns previously reported by Engel *et al* (2001) and Thornber and Gaines (2003). It was thus possible to determine the most efficient potential demographic driver of such spatial variability. This exercise was intended to be generic and not to replace or validate the findings by these authors about their specific subjects. Those were the available data sets on the H:D geographical variability and were taken as a measure of what can be expected to occur in natural populations. It was not surprisingly that only about 5% to 10% of dissimilarity between ploidy phases, imposed over survival rates in survival dominated life-strategies, were enough to generate an H:D variability similar to those reported by Engel *et al* (2001) and Thornber and Gaines (2003). On the other hand, it was necessary to impose around 300% to 550% dissimilarity of fertility rates (dx_{max}) between ploidy phases in fertility dominated life-strategies, to

generate an H:D spatial variability similar to the ones obtained by Thornber and Gaines (2003), and around 83% dissimilarity (dx_{max}) to generate an H:D spatial variability similar to the ones obtained by Engel *et al* (2001). Supporting our findings that a conditional differentiation of survival rates between haploids and diploids is the most efficient (and thus likelier) demographic process to explain the spatial variability of H:D, Thornber and Gaines (2004) found that the spatial variability of the H:D of *Mazzaella flaccida* was positively correlated with the ratio of diploid:haploid mean three month mortality rates ($r=0.96$ and $p=0.003$). It contrasted with the spatial variability of the H:D being uncorrelated with the ratio of diploid:haploid fecundity rates ($r=0.1$ and $p=0.8$). This conditional differentiation set by ploidy dissimilar mortality rates was earlier pointed out as essential for the stability and evolution of biphasic life cycles (Hughes and Otto, 1999). On the other hand, neither mortality nor fecundity rates could explain the observed H:D variations of *M. laminarioides* (Thornber and Gaines, 2004). Likewise, Engel *et al* (2001) found neither fecundity nor survival of *Gracilaria gracilis* exhibited statistically significant ploidy phase dissimilarities. Nevertheless, the 5% and 5.5% dissimilarities in survival rates may be subtle enough to become veiled by background noise in a statistical analysis but still influence the H:D variability; whereas it is unlikely that 83% and 300% dissimilarities in fertility rates become veiled by background noise. Ploidy dissimilarities in survival or fertility rates are only two potential drives for observed H:D variabilities. It is also possible for the drives to be in some other factor that was not caught by the biological, spatial and/or temporal resolution of the models and analysis. It would justify mismatches between the predicted ploidy dissimilarities and the field observations.

The hypothesis that ploidy phase dissimilarities of survival rates are the drive for uneven H:Ds has been sometimes dismissed (Fierst *et al* 2005, Gonzalez and Meneses 1996), possibly because evidences of such dissimilarities have been found to be low and statistically not significant (Destombe *et al* 1989, Engel *et al* 2001, Thornber and Gaines 2004). For example, Fierst *et al* (2005) considered that phase dominance may not result from phase specific adaptations that confer different mortality rates. In contrast, it was showed in the previous chapter that very small differences between ploidy phases in the survival related rates have a much higher potential to generate an uneven H:D than much higher fertility rate differences between ploidy phases. The present work further shows that if the dissimilarities of

survival related rates change with spatial location, even at very low levels, they can determine high H:D spatial variability, which fertility rates can not.

It is noteworthy that even though the spatial variability of the H:D is mostly driven by conditional differentiation of the survival rates, the average values of the H:D is likely to be set by ploidy phase dissimilarities of fecundity rates. This was patent in this work when fecundity had to be manipulated to adjust the average H:D to the values observed in natural populations. A high dissimilarity between haploid and diploid fecundity was necessary to impose to the models. This was first suggested by Thornber and Gaines (2004), who showed that a higher diploid fecundity was the drive for the average haploid dominance in *Mazzaella flaccida*, while the observed spatial variability in the H:D could only be explained by differences in mortality rates.